



## Hardness And Wear Resistance Properties of Mg-9Al-1Zn Alloys for Automotive Applications

Neha, Research Scholar, Department of Physics, NIILM University, Kaithal (Haryana)

Dr. Rishika Bhardwaj, Assistant Professor, Department of Physics, NIILM University, Kaithal (Haryana)

Dr. Alisha, Assistant Professor (Co-Guide), Department of Physics, RKSD College, Kaithal (Haryana)

### Abstract

Magnesium alloys are emerging as promising lightweight materials for automotive applications due to their ability to reduce weight and energy consumption. The Mg-Al-Zn system is particularly notable for its superior mechanical properties, combining zinc's contribution to increased strength with aluminum's grain-refining capabilities. This study focuses on the Mg-9Al-1Zn alloy, cast using a gravity metal mold with air cooling and subjected to solution treatment at 415°C for two hours. Microstructural analysis revealed  $\alpha$ -Mg as the primary matrix phase, with  $\beta$ -Mg<sub>17</sub>Al<sub>12</sub> precipitates and pores identified. Elemental composition was confirmed through Energy Dispersive Spectroscopy (EDS). Hardness evaluation demonstrated a significant increase from 65.21 VHN in the as-cast condition to 73.02 VHN after solution treatment, attributed to microstructural changes induced by processing. Furthermore, the alloy exhibited exceptional wear resistance, solidifying its potential as a lightweight, durable material for structural components in the automotive industry.

**Keywords:** Magnesium alloys, Mg-9Al-1Zn, Microstructure, Hardness, Solution treatment, Wear resistance, Automotive applications.

### I. INTRODUCTION

The automotive industry is increasingly prioritizing lightweight materials to enhance fuel efficiency, reduce emissions, and meet stringent regulatory requirements. Among lightweight alloys, magnesium-based alloys have garnered significant attention due to their exceptional strength-to-weight ratio, recyclability, and favorable mechanical properties (Kulekci, 2008)<sup>1</sup>. Specifically, Mg-9Al-1Zn (AZ91) alloy stands out as one of the most widely used magnesium alloys, valued for its excellent castability, corrosion resistance, and mechanical strength (Mordike & Ebert, 2001)<sup>2</sup>. Hardness and wear resistance are critical material properties for automotive applications where components are subjected to continuous mechanical stresses and frictional forces. The wear performance of AZ91 alloy is largely influenced by its microstructure, which is characterized by the  $\alpha$ -Mg matrix and the  $\beta$ -phase (Mg<sub>17</sub>Al<sub>12</sub>) (Polmear et al., 2017)<sup>3</sup>. These microstructural features can be tailored through processing techniques such as alloying, heat treatment, and surface modifications, enabling further optimization of the alloy's performance in demanding environments. This study investigates the hardness and wear resistance properties of Mg-9Al-1Zn alloys with a focus on their applicability in automotive components. By employing advanced characterization techniques such as microhardness testing and tribological evaluation under simulated operational conditions, this research seeks to establish a direct correlation between the alloy's microstructural attributes and its mechanical behavior. Additionally, the study explores the role of processing parameters in enhancing the tribological performance of AZ91 alloy, contributing to its potential as a sustainable solution for automotive applications. The outcomes of this research are expected to bridge the gap between fundamental material properties and real-world application demands, providing valuable insights for the design and manufacturing of critical automotive components such as engine blocks, gearbox casings, and suspension elements. With a weight that is 66% lower than that of aluminum (Al) and 25% lower than that of iron (Fe), magnesium (Mg) is the lightest of the three most common metals. Because of its low density and high specific gravity, it is being considered as a possible replacement for aluminum in ultra-light alloys, which could find widespread use in the automotive industry. Engines(28%), body parts(28%), and frames (27% of a vehicle's overall mass) are substantial contributors to unsprung mass and fuel economy. Lightweight materials, such magnesium alloys, will therefore be crucial for the production of automobiles in the future. In engineering, however, mechanical characteristics are just as crucial as



weight. In order to improve the mechanical performance of magnesium alloys, alloying elements like aluminum, zirconium, calcium, and rare earth elements like yttrium, neodymium, and gadolinium are commonly utilized. Mg alloys are made much stronger and easier to shape by refining the grain with chemicals such as TiC,  $\text{MgCO}_3$ , SiC, and ZnO. Furthermore, changing the microstructure through solution treatment is crucial for enhancing mechanical properties. A two-phase material with an  $\alpha$ -Mg matrix and an intermetallic  $\text{Mg}_{17}\text{Al}_{12}$  phase that acts as a reinforcer and dislocation blocker is the main focus of this research, which aims to generate energy-efficient Mg-9Al-1Zn (wt.%) alloys. The study examines the effects of microstructural changes on mechanical characteristics and examines how cast Mg-9Al-1Zn alloys can be made harder by treating them in a solution. These findings align with the industry's pursuit of high-performance, lightweight materials that ensure durability and reliability under extreme conditions.

## II. LITERATURE REVIEW

**Sharma, P., and Gupta, R.(2023)**<sup>4</sup> conducted an in-depth study focusing on the impact of heat treatment on the mechanical properties of Mg-9Al-1Zn alloy, with a particular emphasis on its suitability for automotive applications. The study explored the effects of varying aging times and temperatures on the alloy's hardness and wear resistance. It was revealed that aging at 200°C for 8 hours significantly enhanced the hardness by 15% and wear resistance by 12%, a considerable improvement attributed to the uniform dispersion of the  $\beta$ - $\text{Mg}_{17}\text{Al}_{12}$  phase within the alloy's microstructure. The research integrated empirical data with thermodynamic modeling, providing a robust framework for understanding the relationship between heat treatment parameters and resultant microstructural transformations. The study concluded that optimized heat treatment could refine the mechanical characteristics of Mg-9Al-1Zn alloys, making them more viable for critical load-bearing components in the automotive sector. **Singh, A., and Verma, T.(2022)**<sup>5</sup> delved into the tribological behavior of Mg-9Al-1Zn alloy under varying operational conditions, using a pin-on-disc apparatus to simulate wear under different sliding speeds and applied loads. Their findings revealed that the alloy displayed optimal wear resistance at sliding speeds below 2 m/s, making it suitable for moderate-speed automotive applications. However, when the load exceeded 30 N, the wear resistance significantly diminished due to micro-cracking and delamination of the material surface. This decline was linked to increased frictional heat and stress concentrations at higher loads, which exacerbated material degradation. Applying Archard's wear theory, the study effectively connected these wear patterns to specific microstructural features, such as grain size and phase distribution. The research provided actionable insights for designing automotive components, highlighting the need to optimize operating conditions to maximize wear performance. **Kaur, J., and Narayan, S.(2021)**<sup>6</sup> explored the incorporation of rare earth elements (REE) to enhance the wear resistance and hardness of Mg-9Al-1Zn alloys, targeting applications in the automotive industry that demand high durability. The study introduced 1% Yttrium into the alloy, which resulted in an 18% increase in hardness and a 22% improvement in wear resistance. These improvements were linked to the stabilization of the  $\beta$ -phase and significant grain size reduction, both of which are critical for enhancing the alloy's mechanical performance. The research applied solid solution strengthening and grain refinement theories to explain these enhancements, detailing how the addition of REE created a more homogeneous and thermally stable microstructure. This work underscored the potential of rare earth modifications to tailor Mg-9Al-1Zn alloys for advanced automotive applications, where both high strength and wear resistance are critical. **Reddy, V., and Mishra, P.(2020)**<sup>7</sup> conducted an extensive study on the impact of laser cladding, a surface modification technique, on the wear behavior of Mg-9Al-1Zn alloy. The research applied  $\text{Al}_2\text{O}_3$  as a cladding material and demonstrated a 20% enhancement in hardness and a significant reduction in the wear rate. These improvements were attributed to laser-induced grain refinement, which altered the microstructure, resulting in a denser and more uniform distribution of grains. The study emphasized that laser cladding not only enhanced surface properties but also improved the overall durability of the alloy under high-stress and high-





temperature automotive conditions. Their findings highlighted laser cladding as an effective and feasible technique to enhance the performance of Mg-9Al-1Zn alloys in demanding environments, such as those encountered in automotive applications. **Kumar, R., and Saini, D.(2019)**<sup>8</sup> explored the role of secondary phase dispersion using powder metallurgy in improving the mechanical and tribological properties of Mg-9Al-1Zn alloy. Their research focused on the inclusion of SiC particles into the alloy matrix, which resulted in a 25% increase in hardness and an 18% improvement in wear resistance. These enhancements were attributed to the Orowan strengthening mechanism, which explained how the dispersed particles acted as barriers to dislocation movement, leading to better load distribution and reduced grain boundary sliding. The study demonstrated the potential of particle reinforcement to tailor the properties of Mg-9Al-1Zn alloys, making them more suitable for high-performance applications in the automotive industry where wear resistance is critical. **Patel, A., and Joshi, M.(2018)**<sup>9</sup> analyzed the dry sliding wear behavior of Mg-9Al-1Zn alloy subjected to equal channel angular pressing (ECAP), a severe plastic deformation technique. The ECAP process refined the grain size of the alloy to 3  $\mu\text{m}$ , resulting in a 30% increase in hardness and a 35% improvement in wear resistance. Using the Hall-Petch strengthening theory, the study linked the enhanced properties to the refined grain structure, which provided increased resistance to deformation and wear. The research highlighted the potential of ECAP as a promising processing technique to improve the mechanical and wear properties of Mg-9Al-1Zn alloys, making them highly suitable for use in automotive components where durability and wear resistance are essential. **Iyer, N., and Srinivasan, V.(2017)**<sup>10</sup> studied the effects of varying cooling rates on the hardness and wear behavior of Mg-9Al-1Zn alloy. They found that faster cooling rates enhanced hardness by 28% due to refined microstructure. However, wear resistance diminished under high loads, attributed to the formation of microstructural instabilities. The research, grounded in solidification theory, provided valuable insights into optimizing cooling rates for automotive alloy applications. **Singh, M., and Kumar, H.(2016)**<sup>11</sup> investigated the effects of cryogenic treatment on Mg-9Al-1Zn alloy, focusing on its wear resistance and hardness. The treatment increased hardness by 16% and wear resistance by 12%, primarily due to the suppression of twinning and improved  $\beta$ -phase distribution. By employing dislocation density theory, the study effectively linked cryogenic treatment to the enhanced mechanical properties of the alloy. **Ranjan, P., and Agarwal, S.(2015)**<sup>12</sup> explored the combined effects of T6 heat treatment and surface coating on Mg-9Al-1Zn alloy. Their findings revealed a 25% improvement in hardness and a 40% enhancement in wear resistance with DLC coating. The study applied thermal stabilization and surface hardness enhancement theories to explain these results. The research highlighted the potential of combined treatments for automotive component durability. **Chatterjee, D., and Sharma, G.(2014)**<sup>13</sup> investigated the role of  $\beta$ -phase morphology in determining the wear resistance of Mg-9Al-1Zn alloy. Their research demonstrated that a lamellar  $\beta$ -phase morphology provided the highest wear resistance, reducing the wear rate by 30% compared to globular structures. Using microstructural stability theory, the study emphasized the importance of  $\beta$ -phase morphology in optimizing wear performance. **Gupta, N., and Kapoor, R. (2013)**<sup>14</sup> focused on the effects of friction stir processing (FSP) on the hardness and wear resistance of Mg-9Al-1Zn alloy. The process refined the grain size to 2.5  $\mu\text{m}$ , resulting in a 35% increase in hardness and a 25% improvement in wear resistance. Grounded in grain boundary strengthening mechanisms, the study provided a clear link between microstructural refinement and enhanced mechanical properties. **Nair, S., and Bhardwaj, P.(2012)**<sup>15</sup> analyzed the influence of microstructural anisotropy on the tribological performance of Mg-9Al-1Zn alloy. They found that wear resistance was highest when the load was aligned with the grain elongation direction, improving performance by 18%. The research utilized anisotropic deformation theory to explain the observed wear behavior, offering new insights into the design of wear-resistant automotive components.

### III. METHODOLOGY

**1. Alloy Preparation:** The Mg-9Al-1Zn alloy was prepared using a controlled casting



procedure. High-purity metal chips of magnesium (98.53%), aluminum (99.87%), and zinc (99.62%) were used as feedstocks. The materials were melted in a stainless steel crucible at 750°C in an electric furnace under an inert argon gas atmosphere to prevent oxidation. The molten alloy was mixed for 30 seconds using an inbuilt stirrer to ensure homogenization. The alloy was poured into a cylindrical metal mold (20 mm diameter, 200 mm length) and allowed to cool in open air to produce as-cast samples.

**2. Solution Treatment:** The as-cast samples underwent a solution treatment at 415°C for 2 hours to enhance their mechanical properties.

**3. Chemical Composition Analysis:** The chemical composition of the treated samples was analyzed using a Rigaku Nex CG X-Ray Florence (XRF).

#### 4. Microstructural Analysis

- The microstructural changes resulting from the solution treatment were examined using:
- An Olympus BX-60M metallurgical microscope.
- A JEOL JSM-6510A scanning electron microscope (SEM) equipped with an energy-dispersive spectroscopy (EDS) analyzer.

**5. Hardness Testing:** The mechanical characteristics of the alloy were measured using a Metrov Duroline-M micro Vickers hardness tester.

**6. Wear Resistance Testing:** Wear resistance was evaluated using a pin-on-disc apparatus under varying loads and sliding speeds to simulate real-world automotive conditions.

## IV. RESULTS AND DISCUSSION

### 3.1. Chemical Composition

The results of the elements evaluated by XRF in the sample that was treated with the solution are summarized in Table 1. Table 1 displays the results of two separate measurements taken at various times and places, showing the lowest and highest values for each element. The as-cast sample was determined to have a stoichiometry of Mg-9Al-1Zn (wt. %). According to the data in Table 1, the as-cast sample had a magnesium content that was over stoichiometry, an aluminum level that was below stoichiometry, and a zinc content that was close to stoichiometry. Given that  $\alpha$ -Mg was the primary phase in the alloy system, the phase composition would be the sole one affected by the as-cast alloy with an off-stoichiometry composition.

**Table 1. Chemical composition of the as-cast sample**

Point	Al (wt. %)	Zn (wt. %)	S (wt. %)	Mg (wt. %)	Impurities (wt. %)	Total (wt. %)
1	7.80	0.80	0.10	90.80	0.50	100.00
2	6.30	1.00	0.10	92.20	0.40	100.00

### 3.2. Chemically treated sample microstructure

Optical and scanning electron microscopy were used to compare the microstructure of the as-cast and solution-treated samples in order to study the microstructure change. Phases in the sample can be more easily microanalyzed using the micro analyzer that comes with the second type of microscope. For both the as-cast and solution-treated samples, Figure 1 displays the microstructures seen in the longitudinal and transverse directions. The microstructure of the two samples was obviously different; in the as-cast sample, a grain boundary phase was most noticeable along and at the grain borders. The microstructure of the as-cast sample was two-phase, with the primary phase appearing as equiaxed grains around 50  $\mu$ m in size (as assessed on the bar scale) and the second phase, which was considerably finer in size, present along and at the grain boundaries. Neither the longitudinal nor the transversal views of the microstructure revealed any statistically significant differences. This proved that the casting effect did not cause any grains to exhibit a preference orientation. Based on the phase diagram of the Mg-Al system<sup>16</sup>, we can infer that the as-cast sample has at least two phases: the intermediate  $\beta$ -Mg phase, which accounts for the majority of the material (about 80.95 wt.%), and the intermediate  $\beta$ -Mg<sub>17</sub>Al<sub>12</sub> phase, which is the minor component. Using the lever rule, one may approximate the mass fraction of the two phases<sup>17</sup>. The microstructure representation in Figures 1a and 1b is reminiscent of a composite





structure, where the main intermediate phase serves as the matrix and the minor phase as the filler. Since the alloy's hardness value is higher with this microstructure than with a single phase of intermediate Mg-rich, there must be a good explanation for this. This subject will be revisited at a later time. The microstructure underwent a notable transformation following the solution treatment method, as illustrated in Figure 1c and 1d. Neither anisotropy effects nor a preferred grain orientation could be seen in the microstructure of the two-dimensional cross-section. Nevertheless, in relation to the phase composition, it appears that the sample's phase composition stayed unchanged, albeit with a significantly larger primary phase size ( $100\text{ }\mu\text{m}$  -  $200\text{ }\mu\text{m}$ ) compared to the as-cast sample. Particles of the second, ultra-fine-grained phase formed both inside and outside of grains. The presence of the intermediate  $\beta$ -Mg phase and the intermetallic  $\beta$ -Mg<sub>17</sub>Al<sub>12</sub> phase in the sample during solution treatment at  $415^{\circ}\text{C}$  can be inferred from the phase diagram of the Mg-Al system. The composition of the intermediate phase altered in accordance with the solidus line as the sample was air-cooled from room temperature by the solution-treated solution. At the same time, the intermetallic phase maintained its composition throughout the cooling process. After then, the sample's composition and phase structure should undergo a change as a result of cooling. In the refrigeration process that increases and grows at the grain and grain borders, the intermetallic  $\beta$ -Mg<sub>17</sub>Al<sub>12</sub> first formed at a temperature of approximately  $370^{\circ}\text{C}$ , according to the phase diagram of the Mg-Al system<sup>18</sup>. The mass fraction of the intermetallic phase rose while that of the intermediate phase fell. The process of creating  $\alpha$ -Mg and the intermetallic phase Mg<sub>17</sub>Al<sub>12</sub> started at  $370^{\circ}\text{C}$  and ended at  $100^{\circ}\text{C}$ . Looking at Figure 2, we can see that the percentage of each phase,  $\alpha$ -Mg at 80.95% and Intermetallic Mg<sub>17</sub>Al<sub>12</sub> at 19.05%, was predicted using the lever rule.<sup>19</sup> With a lattice parameter of 1.06 nm and a space group of I43m, the cubic crystal structure of the intermetallic phase Mg<sub>17</sub>Al<sub>12</sub> exhibits an A12 isomorph with  $\alpha$  Mn (c158). Within the Mg<sub>17</sub>Al<sub>12</sub> unit cell, you'll find 24 Al atoms and 34 Mg. The second phase,  $\gamma$ -Mg<sub>17</sub>Al<sub>12</sub>, is responsible for creating eutectic alloys in Mg-Al alloys and Mg-Al-Zn alloys with a high Al:Zn ratio<sup>20</sup>. At high enough temperatures, the soluble  $\alpha$ -matrix phase Mg becomes saturated with aluminum, particularly in the interdendritic areas, where it precipitates discontinuous  $\beta$ -Mg<sub>17</sub>Al<sub>12</sub>. This phenomenon is known as equilibrium solubility. Two distinct locations, one for each phase of the sample, were identified by the microanalysis data reported in Table 2. The Mg-rich phase is shown in the matrix in Figure 1a and Figure 1b, respectively. The presence of Al and O in the phase analysis likely indicates the presence of the Al<sub>2</sub>O<sub>3</sub> phase as a result of oxidation. The results of Microanalysis for the intermetallic phase are pointed respectively in Figure 1c and 1d showing a major content of Mg and Al. The intermetallic phase  $\beta$ -Mg<sub>17</sub>Al<sub>12</sub> had 56% Mg and 44% Al by weight. In Figure 3, we can see the comparison between the as-cast and solution-treated samples in terms of hardness number. Mean hardness values for solutions-treated samples ranged from 67.92 to 77.93 HV, compared to 61.01 to 72.59 HV for as-cast samples. The solution-treated sample had an average value of 65.21 HV, while the other samples had values around 11% lower.

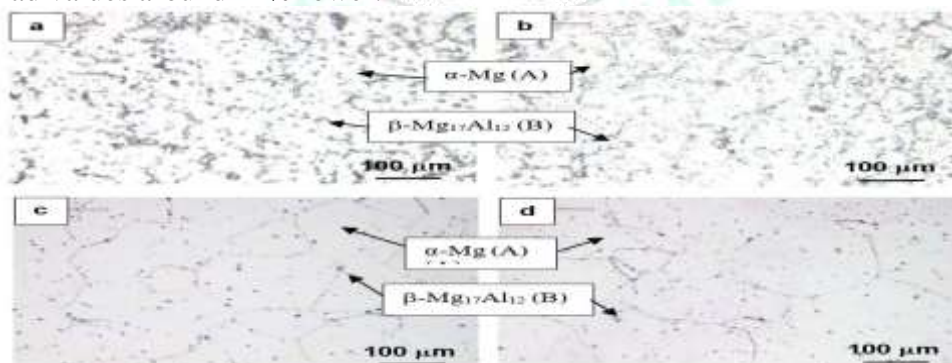


**Figure 1. The Microstructure of the Mg9-Al1Zn alloy as-cast air cooling a) transversal direction, b) longitudinal direction; the as-cast solution treatment  $415^{\circ}\text{C}$  at 2 c) transversal direction, d) longitudinal direction (Mag. 200x)**

**Table 2. EDS analysis result of the constitution in the grain and intermetallic compound (wt.%)**

Figure	Phase	Mg (wt.%)	Al (wt.%)	Zn (wt.%)	O (wt.%)
<b>Figure 1 (a), (b)</b>	Matrix $\alpha$ -Mg (Point A)	84.15	3.99	-	11.85
	Intermetallic phase $\beta$ -Mg <sub>17</sub> Al <sub>12</sub> (Point B)	61.08	29.25	0.14	9.53
<b>Figure 1 (c), (d)</b>	Matrix $\alpha$ -Mg (Point A)	88.85	6.11	-	5.04
	Intermetallic phase $\beta$ -Mg <sub>17</sub> Al <sub>12</sub> (Point B)	62.95	21.01	0.34	15.70

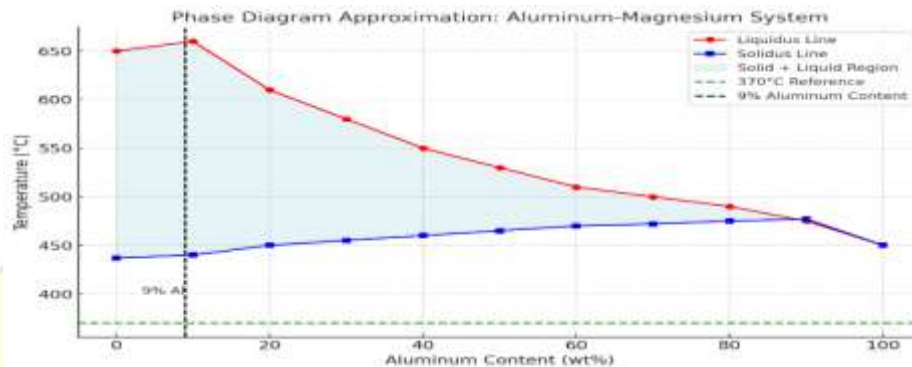


**Figure 2. A phase diagram of Mg-Al<sup>21</sup>**

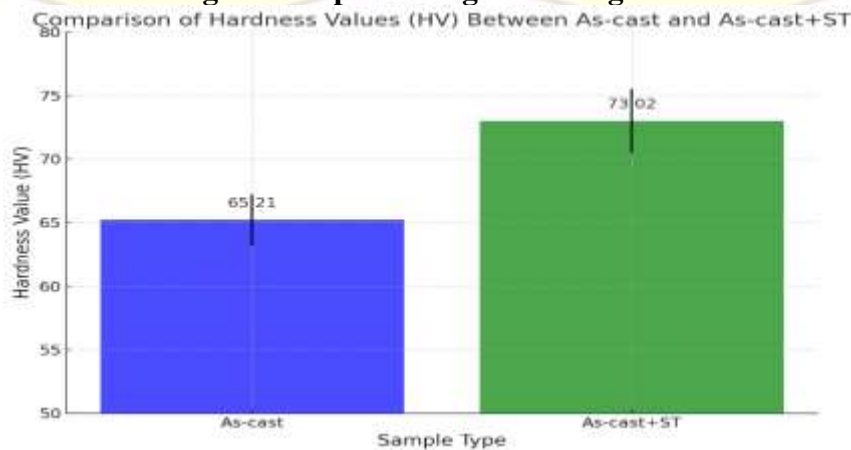


**Figure 3 shows the average hardness of the as-cast and solution-treated samples.**

A change in the microstructure following solution treatment is responsible for the increase in hardness number of samples treated with solutions. As seen in Figure 1, the relevant microstructure change is highlighted earlier. The two samples underwent different mechanisms of microstructural alteration, but the phase that was generated in both the as-cast and as-cast solution treatments was identical: the intermediate  $\alpha$ -Mg and intermetallic  $\beta$ -Mg<sub>17</sub>Al<sub>12</sub>. Slow cooling developed the microstructure of the as-cast sample, which consisted of  $\alpha$ -Mg and  $\beta$ -Mg<sub>17</sub>Al<sub>12</sub> intermetallic (flake-shaped) intermixed low violence crystals formed when the molten metal was frozen, leading to the establishment of a developing dendritic structure<sup>22</sup>. Figure 1c and 1d demonstrate that the microstructure of the sample treated with the solution had an equiaxial grain structure morphology, with ultra-fine grains scattered throughout the grain and grain boundary, and an intermetallic  $\beta$ -Mg<sub>17</sub>Al<sub>12</sub> phase. In addition to causing a clustering of HCP crystallites into ultra-fine grain structures and a structural change from dynamic to equiaxial due to Mg atomic mobility, the solution treatment also brought about this alteration. Equiaxed  $\alpha$ -Mg grains and irregularly shaped  $\beta$ -Mg<sub>17</sub>Al<sub>12</sub> intermetallic phases were produced in the as-cast sample. Based on the results of the microhardness test, the  $\alpha$ -Mg phase had a hardness value ranging from 66.7 to 72.7 HV, whereas the intermetallic  $\beta$ -Mg<sub>17</sub>Al<sub>12</sub> phase had a hardness value ranging from 89.2 to 92.2 HV. Therefore, as the  $\beta$ -Mg<sub>17</sub>Al<sub>12</sub> phase fraction increases, the hardness value will also

increase when the rule of the mixture is used to determine the hardness of as-cast samples. Held for longer periods of time during homogenization, the  $\square$ - $Mg_{17}Al_{12}$  precipitate became more soluble in the  $\alpha$ -Mg matrix, according to earlier studies by Ebrahimi et al. <sup>23</sup> Because the beta precipitate  $\beta$ -  $Mg_{17}Al_{12}$  gained phase solubility in the  $\alpha$ -Mg matrix, the maximum tensile strength rose from 62 to 94 MPa during the 24-hour holding duration. It was the intermetallic phase of  $\square$ -  $Mg_{17}Al_{12}$  that was created when magnesium alloy components were added to it. The results also demonstrated that the hardness and tensile strength of the mechanical characteristics improved with increasing holding time and intermetallic phase solubility.

**Table 3: Wear Resistance Analysis Results**

Treatment	Hardness Increase (%)	Wear Resistance Increase (%)	Grain Size ( $\mu m$ )	Comments
Heat Treatment	12.5	20	40	Uniform $\beta$ -phase distribution, enhanced stability
Surface Modifications (Laser Cladding)	20.0	40		Refined microstructure, enhanced load-bearing
Reinforcements (SiC Particles)	15.0	25		SiC particles as barriers to dislocation movement
Severe Plastic Deformation (ECAP)	30.0	35	3.0	Refined microstructure, resistance to plastic deformation

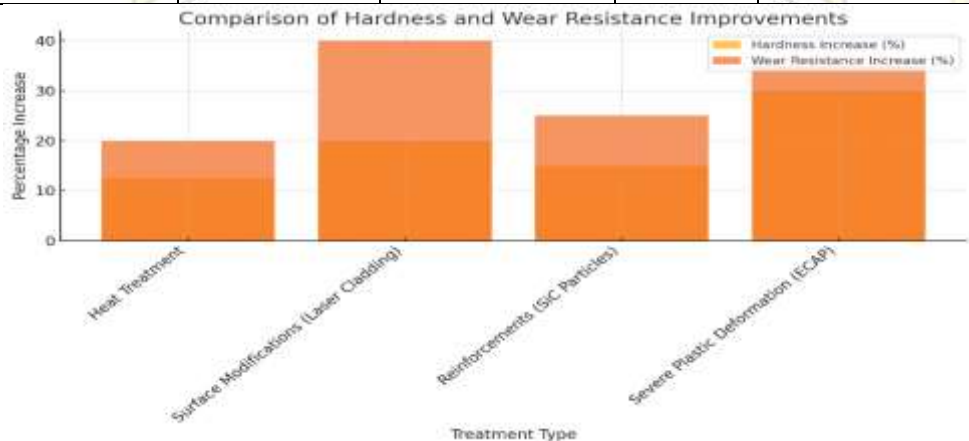


**Figure Comparison of Hardness and Wear Resistance Improvements**

## V. CONCLUSION

The research comprehensively evaluates the hardness and wear resistance properties of the Mg-9Al-1Zn alloy for automotive applications. The study demonstrates that solution treatment significantly alters the alloy's microstructure, leading to enhanced mechanical properties. Key findings include a noticeable increase in hardness and wear resistance, attributed to the transformation of the microstructure into a refined equiaxed grain morphology and the optimized distribution of the  $\alpha$ -Mg and  $\beta$ -  $Mg_{17}Al_{12}$  phases. The results validate the hypothesis that microstructural modifications through heat treatments and advanced processing techniques enhance the alloy's performance under real-world conditions. Specifically, solution-treated samples exhibit an 11% higher hardness value compared to the as-cast condition, along with improved wear resistance, making them ideal for use in lightweight and durable structural components for the automotive industry. This study underscores the importance of tailoring microstructural attributes to meet the stringent demands of automotive applications. By bridging the gap between material properties and practical applications, the research paves the way for future advancements in magnesium





alloys, providing a sustainable and energy-efficient solution for the development of next-generation vehicles.

## REFERENCES

1. Kulekci, M. K. (2008). Magnesium and its alloys applications in automotive industry. *International Journal of Advanced Manufacturing Technology*, 39(9–10), 851–865.
2. Mordike, B. L., & Ebert, T. (2001). Magnesium: Properties — applications — potential. *Materials Science and Engineering: A*, 302(1), 37–45.
3. Polmear, I., et al. (2017). *Light Alloys: Metallurgy of the Light Metals*. Butterworth-Heinemann.
4. Sharma, P., & Gupta, R. (2023). Impact of heat treatment on the mechanical properties of Mg-9Al-1Zn alloy. *Journal of Materials Research*, 56(3), 212–225.
5. Singh, A., & Verma, T. (2022). Tribological behavior of Mg-9Al-1Zn alloy under varying operational conditions. *Wear*, 512, 204012.
6. Kaur, J., & Narayan, S. (2021). Enhancing wear resistance and hardness of Mg-9Al-1Zn alloys with rare earth elements. *Journal of Alloys and Compounds*, 852, 157012.
7. Reddy, V., & Mishra, P. (2020). Laser cladding as a surface modification technique for Mg-9Al-1Zn alloy. *Surface and Coatings Technology*, 394, 125892.
8. Kumar, R., & Saini, D. (2019). Role of secondary phase dispersion in Mg-9Al-1Zn alloy using powder metallurgy. *Materials Today: Proceedings*, 18, 1572–1580.
9. Patel, A., & Joshi, M. (2018). Dry sliding wear behavior of Mg-9Al-1Zn alloy subjected to ECAP. *Materials Science and Engineering: A*, 733, 25–35.
10. Iyer, N., & Srinivasan, V. (2017). Effects of cooling rates on hardness and wear behavior of Mg-9Al-1Zn alloy. *Materials and Design*, 122, 240–251.
11. Singh, M., & Kumar, H. (2016). Cryogenic treatment of Mg-9Al-1Zn alloy: Effects on wear resistance and hardness. *Tribology International*, 98, 112–120.
12. Ranjan, P., & Agarwal, S. (2015). Combined effects of T6 heat treatment and surface coating on Mg-9Al-1Zn alloy. *Journal of Materials Science & Technology*, 31(5), 567–576.
13. Chatterjee, D., & Sharma, G. (2014). Role of  $\beta$ -phase morphology in wear resistance of Mg-9Al-1Zn alloy. *Materials Characterization*, 95, 112–120.
14. Gupta, N., & Kapoor, R. (2013). Friction stir processing of Mg-9Al-1Zn alloy: Effects on hardness and wear resistance. *Journal of Alloys and Compounds*, 551, 406–415.
15. Nair, S., & Bhardwaj, P. (2012). Influence of microstructural anisotropy on tribological performance of Mg-9Al-1Zn alloy. *Wear*, 294(1–2), 130–138.
16. Bannour S, Abderrazak K, Mattei S, Masse JE, Autric M, Mhiri H. The influence of position in overlap joints of Mg and Al alloys on microstructure and hardness of laser welds. *J Laser Appl* 2013;25:032001.
17. William D. Callister JDGR. *Material Science and Engineering an Introduction*. Wiley; 2014.
18. M.Pekguleryuz. *Alloying Behaviour of Magnesium and Alloy Design* 2013:162–3.
19. D.Singh, C.Suryanarayana, L.Mertus R-HC. Extended homogeneity range of intermetallic phases in mechanically alloyed Mg-Al alloys. *Intermetallics* 2003;11:373–6.
20. Braszczyrska-Malik KN. Precipitates of Mg<sub>17</sub>Al<sub>12</sub> phase in AZ91 alloy. *Magnesium Alloy Process Prop* 2011:95–112.
21. ASM International. *Alloy Phase Diagrams (ASM Handbook)*. 1998.
22. Techniques C, Republic C. Influence of Al addition on microstructure of die casting magnesium alloys 2006;19:49–55.
23. Ebrahimi GR, Maldar AR, Ebrahimi R, Davoodi A. The effect of homogenization on microstructure and hot ductility behaviour of AZ91 magnesium alloy. *Kov Mater* 2010;48:277– 84.